ChemComm

COMMUNICATION

View Article Online
View Journal | View Issue

Cite this: *Chem. Commun.*, 2023, 59, 11660

Received 28th July 2023,
Accepted 5th September 2023

DOI: 10.1039/d3cc03634k

rsc.li/chemcomm

Moving into the red – a near infra-red optical probe for analysis of human neutrophil elastase in activated neutrophils and neutrophil extracellular traps†

M. Rodriguez-Rios,[a] G. Rinaldi,[b] A. Megia-Fernandez,[ac] A. Lilienkampf,[a] C. T. Robb,[b] A. G. Rossi[b] and M. Bradley *[d]

Neutrophils are the first immune cells recruited for defence against invading pathogens; however, their dysregulated activation and subsequent release of the enzyme human neutrophil elastase is associated with several, inflammation-based, diseases. Herein, we describe a FRET-based, tri-branched (one quencher, three fluorophores) near infrared probe that provides an intense OFF/ON amplified fluorescence signal for specific detection of human neutrophil elastase. The probe allowed selective detection of activated neutrophils and labelling of neutrophil extracellular traps.

Neutrophils are the most abundant white cells in human blood. They are phagocytic immune cells that provide an early line of defence against pathogens,[1] and apply a wide range of mechanisms to kill pathogens including phagocytosis, neutrophil degranulation, reactive oxygen radical generation,[2] and neutrophil extracellular trap (NET) production during a process termed NETosis.[3] In NETosis, neutrophils extrude their intracellular content (including chromatin and antimicrobial proteins) into the extracellular space, forming NETs to entrap and kill pathogens. However, despite their beneficial role in host defence, overactivation of neutrophils and dysregulated NETosis play pivotal roles in many inflammatory diseases,[4] such as SARS-COV2 where NETs can cause microvascular thrombosis, leading to tissue damage, and organ failure.[5] Of key relevance in neutrophil activity is human neutrophil elastase (hNE), a serine protease that is highly abundant in the granules of neutrophils. This protease is found bound to NETs, and is a validated biomarker for inflammation.[6]

Activity-based probes, which covalently bind to elastase, have allowed accurate cellular localisation of the enzyme and enzyme detection in gel-based assays, but most are "always on" fluorescent probes that can have high background signals when used for cell imaging microscopy and have no signal amplification.[7–9] Probes based on Förster resonance energy transfer (FRET),[10] on the other hand, allow signal amplification (probe turnover) and have been used for the detection of various proteases. Examples of FRET-based probes for elastase[11–13] include FRET-based ratiometric probes[14] and probes for elastase sensing that successfully allowed detection of activated neutrophils and visualisation of NETs.[15] However, the majority of these activity and substrate-based probes for elastase lie within the "green" region (495–570 nm) of the visible spectrum where applications are limited by the high background signals commonly observed in biological tissues[16] as well as by the elevated levels of tissue scattering.[17] Thus, efforts on optical probe development have focused on improving the signal-to-noise ratio, often by moving the fluorescent emission of probes into the near infrared (NIR) window (650–900 nm), driving improvements in tissue penetration, reducing scattering ($1/\lambda^4$) and background signal. Indeed, NIR probes are becoming common in the clinical setting with examples including the tyrosine kinase MET receptor optical probe for thyroid cancer detection,[18] the FDA approved folate receptor targeting probe for ovarian cancer intraoperative imaging,[19,20] and a cathepsin-activated imaging probe that has entered clinical studies for intraoperative breast cancer detection.[21]

Multibranched, substrate-based probes for protease detection offer a powerful means for signal amplification, with reduced background fluorescence when compared to their linear counter parts by virtue of "self-quenching"[22] of identical, close proximity fluorophores and release of multiple fluorescent moieties upon cleavage.[23,24] Herein, we present a tri-

[a] *EaStCHEM School of Chemistry, University of Edinburgh, David Brewster Road, EH9 3FJ Edinburgh, UK*
[b] *University of Edinburgh Centre for Inflammation Research, Queen's Medical Research Institute, 47 Little France Crescent, Edinburgh BioQuarter, Edinburgh EH16 4TJ, UK*
[c] *Organic Chemistry Department, Faculty of Sciences, University of Granada, Avda. Fuente Nueva S/N, 18071, Spain*
[d] *Precision Healthcare University Research Institute, Queen Mary University of London, Empire House, 67-75 New Road, London E1 1HH, UK. E-mail: m.bradley@qmul.ac.uk*

† Electronic supplementary information (ESI) available: Supporting figures and schemes, and experimental procedures. See DOI: https://doi.org/10.1039/d3cc03634k

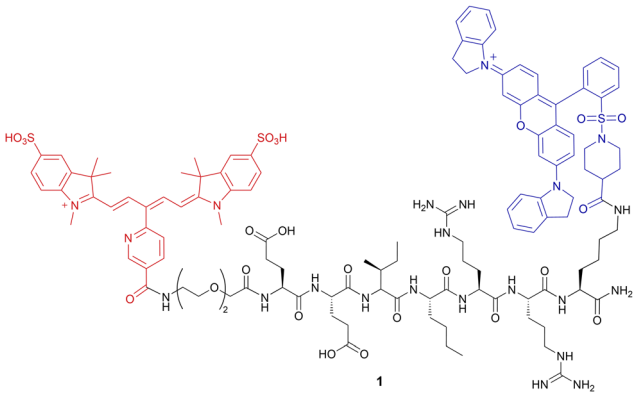

Fig. 1 The structure of the linear FRET-probe **1** (HNE-1F1Q). hNE cleaves the probe between isoleucine and norleucine.

branched NIR probe for hNE that allows the specific detection of the enzyme in activated neutrophils and NETs. The probe was synthesised using a hybrid solid/solution-phase approach, with the final tri-branched construct assembled *via* copper catalysed cycloaddition chemistry.[25,26]

An initial design to explore the desired quencher and fluorophore targeted a classical, linear FRET peptide **1** (HNE-1F1Q) using a sulfonated Cy5 ($\lambda_{ex}/\lambda_{em}$ 640/657 nm) and QSY21 (λ_{abs} 660 nm) FRET pair on opposite ends of a hNE cleavable peptide (Glu-Glu-Ile-Nle-Arg-Arg) (Fig. 1).[13,27] Probe **1** was synthesised on solid-phase using orthogonal Dde/Fmoc deprotection[28] chemistry to allow selective attachment at the lysine side chain of the quencher QSY21 at the C-terminus, with coupling of the Cy5 fluorophore at the amino terminus as the final resin-based step before resin cleavage and deprotection (ESI,† Scheme S1). Surprisingly, when **1** (35 μM) was exposed to hNE, the activation proved to be very slow (>2 h, ESI,† Fig. S1),

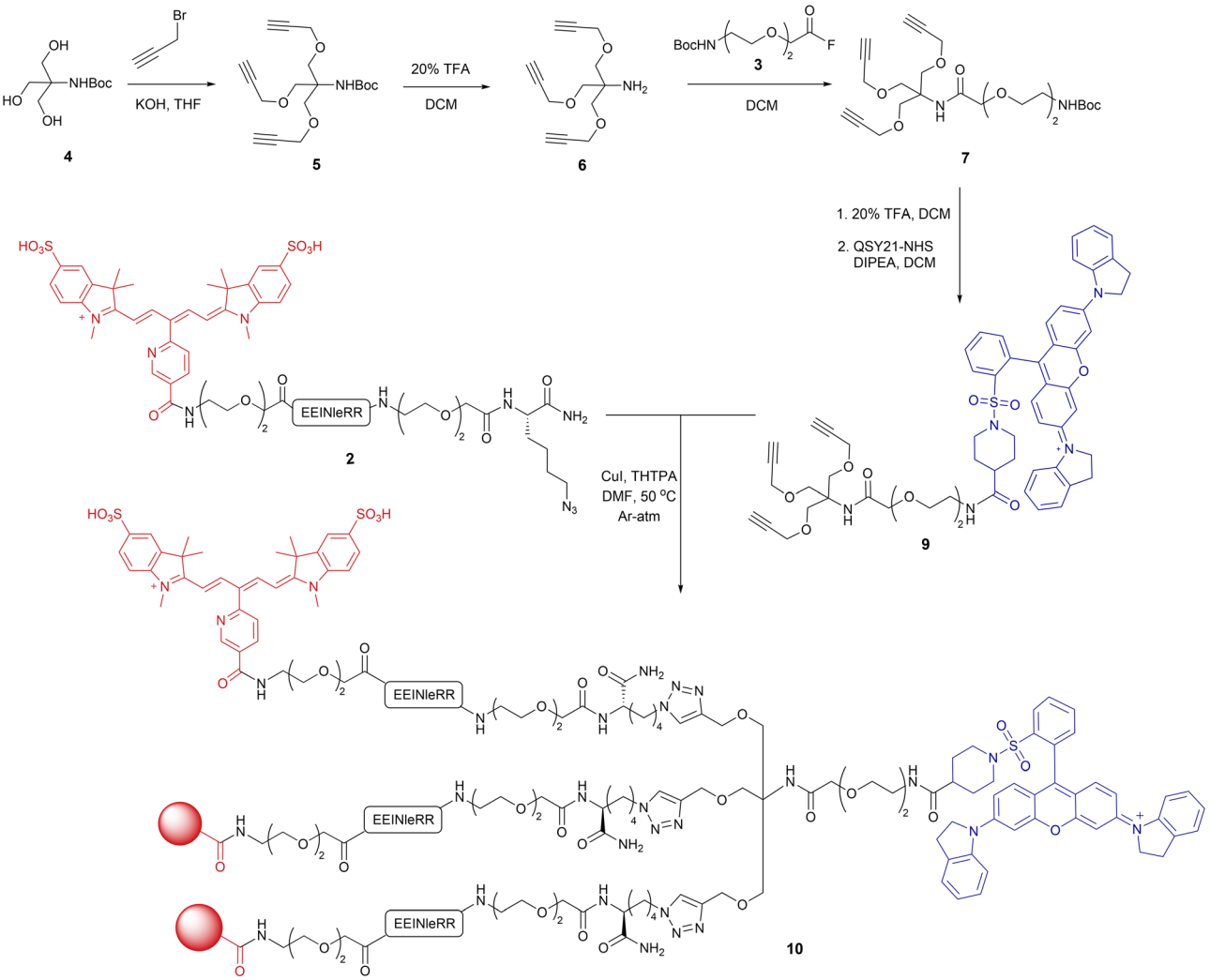

Scheme 1 Synthesis of tri-branched probe **10**. The quencher containing alkyne fragment **9** was synthesised from tris-hydroxymethyl aminomethane in six steps, with an overall yield of 20%. Azide-peptide **2** was synthesised using a Rink-amide linker functionalised polystyrene resin and assembled using standard Fmoc/^{t}Bu SPPS. The azide functionality was incorporated at the C-terminus using Fmoc-Lys(N_3)-OH as the first residue and the peptide was capped with sulfonated Cy5 at its N-terminus (ESI,† Scheme S1). After the copper-catalysed click reaction, the probe was purified by semipreparative HPLC and characterised by MALDI-TOF MS and HRMS.

which was attributed to the bulky quencher hindering enzyme access to the cleavage site and the poor solubility of the probe (precipitation was observed in aqueous buffer even at low concentrations). Also, probe **1** did not show any increase in fluorescence when incubated with activated neutrophils.

To solve these problems, a tri-branched probe **10** was designed, in which a single QSY21 quencher was placed distally to the cleavage site (to improve cleavage kinetics) while using three copies of the sulfonated Cy5-peptide to allow "triple" levels of fluorescence amplification (Scheme 1). In this design, the quencher molecule enhances the overall silencing effect *via* FRET in addition to Cy5 self-quenching. Previously reported solid-phase synthetic methods used for the synthesis of the green emitting tribranched probes[12] for elastase proved unsuccessful and, thus, a new convergent route was designed. The synthesis was achieved by the solid-phase synthesis of the azide-containing peptide **2** (with the N-terminus conjugated to a bis-sulfonated Cy5) on a Rink-amide linker functionalised polystyrene resin. This was followed by the convergent solution-phase attachment of **2** to the tri-branched, QSY21-alkyne scaffold **9** *via* azide/alkyne "click" chemistry (Scheme 1).[29] The tri-branched alkyne scaffold **9** was designed to have the quencher QSY21 attached to the "stem" *via* a bis-ethylene glycol spacer to ease its conjugation. Thus, the hindered amine of the tris-alkyne building block **6**[30] was coupled to the spacer *via* a highly reactive acyl fluoride (Boc-NH-$(EG)_2$-CO-F, **3**). Once the spacer was attached, removal of the Boc group from **7** allowed facile incorporation of QSY21 *via* its NHS ester to give the quencher containing tris-alkyne **9**. The tris-alkyne-QSY21 **9** was then reacted with the azide peptide **2** (4 equiv.) at the highest reactant concentrations possible (limited by solubility – 0.6 mM and 2.5 mM for **9** and **2**, respectively) using CuI/THTPA in anhydrous DMF to give the "three-fluorophores-one-quencher" probe **10** (HNE-3F1Q). Four equivalents of the azide **2** were sufficient for good conversion into the tri-branched compound, with only trace amounts of the mono and bis-functionalised intermediates ever observed by HPLC (ESI,† Fig. S2), suggesting, perhaps, that the mono and dimeric triazole species are catalysts in their own right.

Probe **10** (HNE-3F1Q) had a maximum excitation wavelength (λ_{ex}) at 640 nm and maximum emission (λ_{em}) at 657 nm (Fig. 2a), consistent with the optical properties of the sulfonated Cy5 and, in contrast to the linear FRET probe **1**, was highly water soluble. The probe was "super-silent" in its non-cleaved form, showing that a single QSY21 quencher can efficiently quench the three fluorophores within its proximity, with a rapid increase in fluorescence observed for **10** within seconds of adding hNE, (Fig. 2b), with cleavage occurring at Ile-Nle (Fig S7, ESI†). In comparison, the Cy5 tri-branched control probe **11** (HNE-3F0Q), without the QSY21 quencher, only gave a 2-fold increase in fluorescence upon elastase activation (ESI,† Fig. S3).

The K_M for **10** was 5.7 μM with a turnover number (k_{cat}/K_M) of 3.5×10^4 M^{-1} s^{-1} (ESI,† Fig. S4). The cleavage kinetics of the branched probe **10** were superior to the more traditional, linear FRET peptide **1** (ESI,† Fig. S2–S6), with significantly faster cleavage (k_{cat}/K_M of 1.5×10^3 M^{-1} s^{-1}). The activation of **10**

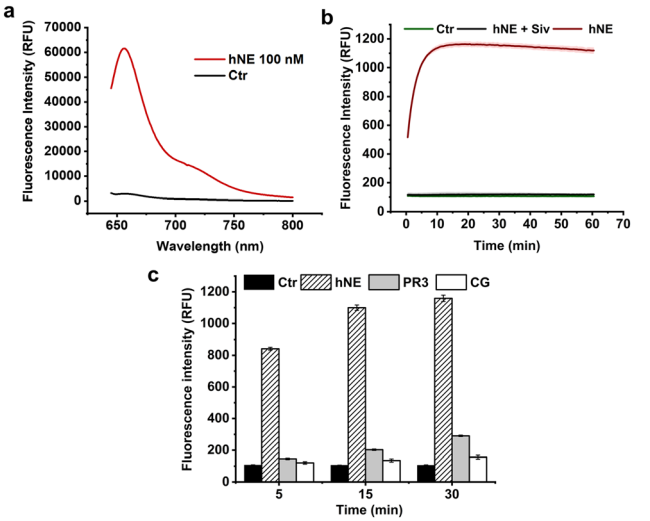

Fig. 2 (a) Fluorescence emission (λ_{ex} = 640/10, λ_{em} = 680/20) of **10** (HNE-3F1Q, 12 μM) after incubation with hNE (100 nM, 1 h) (n = 3, Ctr = no enzyme); (b) time-dependent increase in fluorescence of **10** (12 μM) in the presence of hNE (100 nM). The activation was fully inhibited by the elastase inhibitor sivelestat (100 μM) (n = 3); (c) probe **10** (12 μM) was highly selective for hNE, with negligible cleavage by closely related proteases cathepsin G (100 nM) and proteinase 3 (100 nM) (n =3, Ctr = no enzyme).

was fully inhibited by the elastase inhibitor sivelestat and the probe was highly specific for elastase, with no cleavage by the closely related proteases, proteinase 3 or cathepsin G (Fig. 2c).

To evaluate if **10** (HNE-3F1Q) was able to detect hNE in neutrophils, primary human neutrophils were activated by exposure to two well stablished neutrophil activators *N*-formylmethionyl-leucyl-phenylalanine (fMLF) or phorbol 12-myristate 13-acetate (PMA).[31–33] An increase in fluorescence from cleaved **10** was observed in activated neutrophils when compared to untreated controls that showed negligible fluorescence (Fig. 3). A clear difference between fMLF and PMA activation was observed with fMLF activated neutrophils having intact nuclei while PMA activated cells formed "cloud-like" structures, with the "DNA signal" diffusing into the extracellular environment and co-localised with the NIR signal of **10**, indicating co-localisation of DNA and hNE which is a hallmark feature of NETs. When neutrophils were pre-treated with sivelestat prior to exposure to PMA, no significant increase in fluorescence was observed (Fig S8, ESI†). These results demonstrate that **10** can be used to detect hNE in activated neutrophils and specifically in NETs and that the probe is robust in the absence of the protease.

Detection of hNE in activated neutrophils and NETs was possible with our NIR probe and results were consistent with those obtained with previously reported probes[14,15] that used a similar substrate. However, our results contrasted with findings obtained from Kasperkiewicz[9] that observed that the hNE present in NETs was not active when using phosphonate-based activity-based probes. These contrasting results could be explained by the nature of the probes, with activity-based probes unable to provide signal amplification (and having higher background fluorescence), while substrate-based probes, because they are catalytically activated by the protease, allow for much

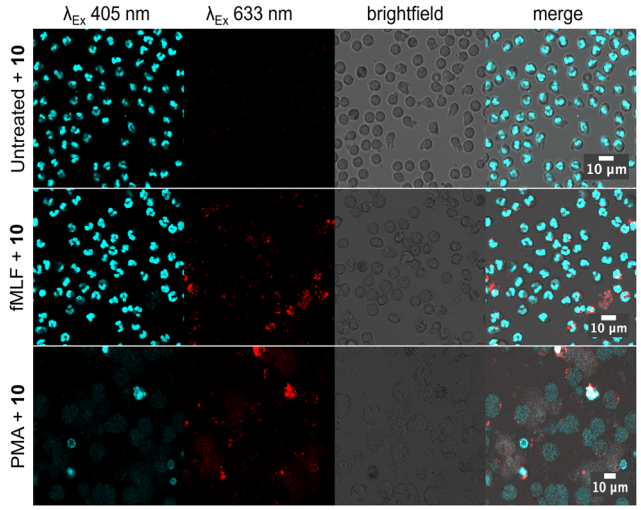

Fig. 3 Fluorescence microscopy images of neutrophils activated with fMLF (100 nM, 30 min) or PMA to induce NETs (10 nM, 3 h) while incubating with probe **10** (3 μM, 3 h), followed by nuclear staining with Hoechst 33342 (200 nM, 20 min). Detection wavelengths: blue channel (Hoechst) λ_{ex} 405 nm, λ_{em} 420–500 nm; red channel (probe) λ_{ex} 633 nm, λ_{em} 650–710 nm.

higher signals and provide lower limits of detection. In addition, activity-based probes lead to inhibition of the protease itself, which could have an effect the NETotic process. It would be interesting to perform a study where both methods of detection are compared side-by-side under the same conditions.

A tri-branched, FRET-based probe for the detection of hNE was synthesised with emission in the NIR region of the spectrum, where endogenous biomolecules have decreased absorbance, and minimal autofluorescence. The probe was synthesised using a convergent assembly method, combining solid-phase peptide synthesis and solution-phase copper catalysed azide/alkyne cycloaddition (CuAAC). Three copies of a sulfonated Cy5 N-terminal labelled elastase substrate, bearing an azide at the C-terminus, were "clicked" by CuAAC onto a tribranched scaffold bearing three terminal alkyne groups and a single copy of the quencher. This strategy allowed the quencher to be placed far from the cleavage site and proved to be key for efficient probe activation. The probe was able to rapidly detect hNE activity *in vitro* and was successfully used to image activated neutrophils and NETs.

We would like to thank Engineering and Physical Sciences Research Council (EPSRC, UK) for Interdisciplinary Research Collaboration grants EP/R005257/1 and Medical Research Council grant MR/N02995X/1.

Conflicts of interest

There are no conflicts to declare.

Notes and references

1 E. Kolaczkowska and P. Kubes, *Nat. Rev. Immunol.*, 2013, **13**, 159–175.
2 P. Lacy, *Allergy, Asthma, Clin. Immunol.*, 2006, **2**, 98.
3 V. Brinkmann, U. Reichard, C. Goosmann, B. Fauler, Y. Uhlemann, D. S. Weiss, Y. Weinrauch and A. Zychlinsky, *Science*, 2004, **303**, 1532–1535.
4 V. Mutua and L. J. Gershwin, *Clin. Rev. Allergy Immunol.*, 2021, **61**, 194–211.
5 Y. Zhu, X. Chen and X. Liu, *Front. Immunol.*, 2022, **13**, 838011.
6 S. J. Thulborn, V. Mistry, C. E. Brightling, K. L. Moffitt, D. Ribeiro and M. Bafadhel, *Respir. Res.*, 2019, **20**, 170.
7 A. C. Schulz-Fincke, M. Blaut, A. Braune and M. Gutschow, *ACS Med. Chem. Lett.*, 2018, **9**, 345–350.
8 S. Y. Liu, H. Xiong, R. R. Li, W. C. Yang and G. F. Yang, *Anal. Chem.*, 2019, **91**, 3877–3884.
9 P. Kasperkiewicza, M. Porebaa, S. J. Snipasb, H. Parkerc, C. C. Winterbournc, G. S. Salvesenb and M. Drag, *Proc. Natl. Acad. Sci. U. S. A.*, 2014, **111**, 2518–2523.
10 M. Rodriguez-Rios, A. Megia-Fernandez, D. J. Norman and M. Bradley, *Chem. Soc. Rev.*, 2022, **51**, 2081–2120.
11 S. Gehrig, M. A. Mall and C. Schultz, *Angew. Chem., Int. Ed.*, 2012, **51**, 6258–6261.
12 S. Kossodo, J. Zhang, K. Groves, G. J. Cuneo, E. Handy, J. Morin, J. Delaney, W. Yared, M. Rajopadhye and J. D. Peterson, *Int. J. Mol. Imaging*, 2011, **2011**, 581406.
13 B. Korkmaz, S. Attucci, M. A. Juliano, T. Kalupov, M. L. Jourdan, L. Juliano and F. Gauthier, *Nat. Protoc.*, 2008, **3**, 991–1000.
14 M. Guerra, V. S. Halls, J. Schatterny, M. Hagner, M. A. Mall and C. Schultz, *J. Am. Chem. Soc.*, 2020, **142**, 20299–20305.
15 M. R. Rios, G. Garoffolo, G. Rinaldi, A. Megia-Fernandez, S. Ferrari, C. T. Robb, A. G. Rossi, M. Pesce and M. Bradley, *Chem. Commun.*, 2020, **57**, 97–100.
16 M. Monici, *Biotechnol. Annu. Rev.*, 2005, **11**, 227–256.
17 J. R. Mourant, J. P. Freyer, A. H. Hielscher, A. A. Eick, D. Shen and T. M. Johnson, *Appl. Opt.*, 1998, **37**, 3586–3593.
18 P. K. C. Jonker, M. J. H. Metman, L. H. J. Sondorp, M. S. Sywak, A. J. Gill, L. Jansen, T. P. Links, P. J. van Diest, T. M. van Ginhoven, C. W. G. M. Löwik, A. H. Nguyen, R. P. Coppes, D. J. Robinson, G. M. van Dam, B. M. van Hemel, R. S. N. Fehrmann and S. Kruijff, *Eur. J. Nucl. Med. Mol. Imaging*, 2022, **49**, 3557–3570.
19 J. L. Tanyi, H. S. Chon, M. A. Morgan, S. K. Chambers, E. S. Han, K. A. Butler, C. L. Langstraat, M. A. Powell, L. M. Randall, A. L. Vahrmeijer, I. S. Winer and R. M. Wenham, *J. Clin. Oncol.*, 2021, **39**, 5503.
20 S. M. Mahalingam, S. A. Kularatne, C. H. Myers, P. Gagare, M. Norshi, X. Liu, S. Singhal and P. S. Low, *J. Med. Chem.*, 2018, **61**, 9637–9646.
21 B. L. Smith, M. A. Gadd, C. R. Lanahan, U. Rai, R. Tang, T. Rice-Stitt, A. L. Merrill, D. B. Strasfeld, J. M. Ferrer, E. F. Brachtel and M. C. Specht, *Breast Cancer Res. Treat.*, 2018, **171**, 413–420.
22 W. Bae, T.-Y. Yoon and C. Jeong, *PLoS One*, 2021, **16**, e0247326.
23 N. Avlonitis, M. Debunne, T. Aslam, N. McDonald, C. Haslett, K. Dhaliwal and M. Bradley, *Org. Biomol. Chem.*, 2013, **11**, 4414–4418.
24 T. H. Craven, N. Avlonitis, N. McDonald, T. Walton, E. Scholefield, A. R. Akram, T. S. Walsh, C. Haslett, M. Bradley and K. Dhaliwal, *Sci. Rep.*, 2018, **8**, 13490.
25 M. Meldal and C. W. Tornøe, *Chem. Rev.*, 2008, **108**, 2952–3015.
26 C. W. Tornøe, C. Christensen and M. Meldal, *J. Org. Chem.*, 2002, **67**, 3057–3064.
27 B. Korkmaz, S. Attucci, E. Hazouard, M. Ferrandière, M. L. Jourdan, M. Brillard-Bourdet, L. Juliano and F. Gauthier, *J. Biol. Chem.*, 2002, **277**, 39074–39081.
28 J. J. Diaz-Mochon and Mark Bradley, *Org. Lett.*, 2004, **6**, 1127–1129.
29 N. J. Agard, J. A. Prescher and C. R. Bertozzi, *J. Am. Chem. Soc.*, 2004, **126**, 15046–15047.
30 Y. M. Chabre, C. Contino-Pépin, V. Placide, T. C. Shiao and R. Roy, *J. Org. Chem.*, 2008, **73**, 5602–5605.
31 H. Takei, A. Araki, H. Watanabe, A. Ichinose and F. Sendo, *J. Leukocyte Biol.*, 1996, **59**, 229–240.
32 A. G. Mahomed and R. Anderson, *Inflammation*, 2000, **24**, 559–569.
33 G. T. Nguyen, E. R. Green and J. Mecsas, *Front. Cell. Infect. Microbiol.*, 2017, **7**, 373.